Available online at www.sciencedirect.com
SCIENCE DIRECT®
Catalysis Today 89 (2004) 297–302
CATALYSIS TODAY
www.elsevier.com/locate/cattod

Elaboration and characterization of the Sr_2FeMoO_6 double perovskite

A. Dinia*, J. Vénuat, S. Colis, G. Pourroy

IPCMS (UMR 7504 du CNRS), ULP-ECPM, 23 rue du Loess, BP 43, F-67034 Strasbourg Cedex 2, France

Abstract

In this work the structural and magneto-transport properties of the Sr_2FeMoO_6 double perovskite prepared using two elaboration processes are presented. The first process is the most used solid-state reaction technique starting from three materials: Fe_2O_3, $SrCO_3$ and metallic MoO_3 with the appropriate amounts. For this process, treatment conditions have been optimized in order to reduce the $SrMoO_4$ amounts in the final compound. The best results have been obtained after annealing the mixture during 1 h at 700 °C under reducing 5% H_2–95% N_2 atmosphere followed by calcinations at 1200 °C under Ar atmosphere during 10 h. X-ray diffraction measurements have shown that the phase can be indexed within the *I4/mmm* space group indicating a tetragonal distortion. The magneto-transport measurements have shown the highest saturation magnetization value reaching 26.7 emu/g at 300 K and a magnetoresistance (MR) of 2.5%. For the second process, the phase has been elaborated using several steps and reacting at each step only two materials. In this case X-ray diffraction shows that the final compound is a single phase with the same space group as for the previous one. In contrast, the saturation magnetization is slightly smaller with 21 emu/g, while, at the opposite, the magnetoresistance is higher reaching 3.6%. These results will be discussed in correlation with the structural results.

Keywords: Sr_2FeMoO_6; Magnetoresistance; Calcination; Half-metallic ferromagnetism

1. Introduction

There is currently a lot of interest in the science and potential technological applications of spin-transport electronics (or spintronics), in which the spin of charge carriers is exploited to provide new functionality for microelectronic devices [1–4]. Spin valves systems and magnetic tunnel junctions have been largely exploited for read/write heads, magnetic sensors and magnetic random access memories. In these systems, the magnetic electrodes are mainly composed of metallic magnetic elements like Co, Fe or CoFe. In order to improve the performance of these electronic devices, it is important to develop new magnetic materials presenting new functionalities at room temperature.

The recent report of colossal magnetoresistance (CMR) at room temperature in Sr_2FeMoO_6 [5] has renewed the interest in magnetic oxides. This effect is attracting considerable interest from both fundamental and practical points of view [6] due to their half-metallic ferromagnetism. Indeed, their Curie temperature T_C can be as high as 415 K in Sr_2FeMoO_6 [5]. In addition to the low field magnetoresistance (MR), this suggests the high spin polarization of conduction electrons.

In spite of the intense research on these magnetic oxides, particularly on Sr_2FeMoO_6, there are still a number of issues that have not been appropriately addressed so far. One of the most striking observations is the systematic presence of parasites phases in the final compound, like $SrMoO_4$. Indeed, it seems that authors did not focus on this point, which is very important, because it indicates that the reaction is incomplete and can partly explain why the saturation magnetization is systematically lower than the predicted value of $M_S = 4\mu_B$. Indeed, the magnetic structure was early described as ferrimagnetic due to antiferromagnetic coupling of B and B′ in the $A_2BB'O_6$ [7]. In Sr_2FeMoO_6, Fe^{3+} spins (d^5; $S = \frac{5}{2}$) are parallely aligned in the B sublattice, and antiferromagnetically coupled to Mo^{5+} (d^1; $S = \frac{1}{2}$) spins, thus leading to $M_S = 4\mu_B$. Another source of the observed lower saturation magnetization can be attributed to the existence of antisite defects in the B/B′ sublattices, i.e. occupation of Fe(Mo) ions in the Mo(Fe) sites [8,9]. In the perfect ordered material (Fig. 1), each Fe ion in the B position is surrounded by six Mo ions at the B′ site. However, when disorder is present, the antiferromagnetic superexchange interaction between nearest neighbor Fe ions reduces the magnetization of the ferromagnetic Fe sublattice, thus reducing M_S.

* Corresponding author. Tel.: +33-3-88-10-70-67; fax: +33-3-88-10-72-49.
E-mail address: aziz.dinia@ipcms.u-strasbg.fr (A. Dinia).

0920-5861/$ – see front matter © 2004 Elsevier B.V. All rights reserved.
doi:10.1016/j.cattod.2003.12.019

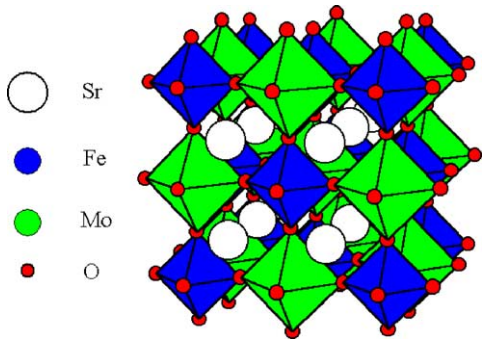

Fig. 1. Schematic view of A2BB′O6 double perovskite, where A is the Sr, B is Fe and B′ is Mo.

The aim of the present work is to develop an elaboration procedure allowing to avoid any parasite phases and leading to a complete reaction. Two processes are reported. The first one is close to what has been widely used, i.e. using the ceramic procedure and starting with stoichiometric compositions of three materials (Fe_2O_3, $SrCO_3$ and metallic MoO_3). Effort has been focused on the reduction procedure in order to optimize the compound. The second one consists of splitting the process in several steps and using for each step only two starting materials. For the first process, X-ray diffraction shows that the amount of $SrMoO_4$ phase can be sensitively reduced but, unfortunately, not eliminated giving for the optimized phase and at room temperature a magnetization at 1.5 T of 26.7 emu/g and a magnetoresistance value of 2.5%. However, the second process allows to eliminate the $SrMoO_4$ phase giving rise to a pure compound but with lower magnetization value at 1.5 T than the previous one.

2. Experimental

The Sr_2FeMoO_6 samples were prepared by solid-state reaction. Two elaboration processes have been used in order to improve the purity of the samples. For the first one, which is close to the protocol used by most of groups, stoichiometric amounts of $SrCO_3$, Fe_2O_3 and MoO_3 were mixed, ground and calcined at 900 °C for 2 h in an Ar atmosphere. The calcined mixtures were reground, pressed and reduced for 1 h under current flow of 5% H_2/95% Ar at 700 °C. Afterwards the mixtures were sintered at 1200 °C under argon flow during 10 h. Unfortunately, the last protocol does not allow to obtain a pure Sr_2FeMoO_6 compound. Indeed, $SrMoO_4$ is thermodynamically favored. Therefore, a segregation occurs which avoid to obtain a pure phase. To get rid of this difficulty, we have developed a sintering process in which only one reaction is performed at each step in order to avoid the formation of $SrMoO_4$. Therefore, in the first step, stoichiometric amounts of $SrCO_3$, Fe_2O_3 were mixed, ground and calcined at 1000 °C during 5 h under an Ar flow giving rise to $Sr_2FeO_{3.5}$ compound. Then stoichiometric amounts of $Sr_2FeO_{3.5,}$ MoO_2 and MoO_3 were mixed, ground, pressed and sintered at 1200 °C during 2 h under N_2/H_2 flow.

Room temperature X-ray diffraction patterns were collected using a Siemens D 500 diffractometer equipped with a primary beam quartz monochromator (Co $K\alpha_1$ = 0.178897 nm).

Magnetizations measurements were performed using a vibrating sample magnetometer in fields up to 1.5 T at 4.2 K and at room temperature.

Magnetoresistance measurements were done at room temperature using the classical four points technique and a Keithly2400 Sourcemeter, and in a magnetic field parallel to the current direction and reaching 1.2 T.

3. Results

3.1. X-ray diffraction

The quality of the samples and their crystallographic structure have been investigated by means of room temperature X-ray diffraction techniques. Fig. 2 shows X-ray diffraction pattern for the optimized sample, labeled A, obtained by the first sintering process. It is clearly observed that in addition to the Bragg peaks of the Sr_2FeMoO_6 phase, additional Bragg peaks occur corresponding to the $SrMoO_4$ phase. A quantitative analysis of all observed Bragg peaks shows that the amount of the $SrMoO_4$ impurity phase is of about 5%. This will have a sensitive consequence on the magneto-transport properties as will be confirmed later. The Rietveld profile analysis has allowed to fit the X-ray spectrum in the *I4/mmm* space group with the cell parameters values of $a = b = 0.55767(7)$ nm and $c = 0.78767(8)$ nm in close agreements with those reported in [5,10,11]. Such results indicate that there is a slight tetragonal distortion with respect to the cubic perovskite.

Fig. 3 shows the X-ray diffraction pattern recorded at room temperature for the sample, labeled B, obtained by the second sintering process. In contrast with the last spectrum, this one seems to show only Bragg peaks corresponding to the Sr_2FeMoO_6 compound. However, there is a very small peak that is hardly distinguishable on the figure at $2\theta = 52°$ and represents a quantity which is smaller than 1% of impurity phase. Unfortunately, we do not success to identify the nature of this phase. The Rietveld profile analysis indicates that the pattern can be successfully fitted using the I4/mmm space group with a similar tetragonal distortion as for the sample A. The cell parameters deduced from this fit are $a = b = 0.55883(5)$ nm and $c = 0.78894(7)$ nm.

3.2. Magnetization

In order to complete the last analysis and to have more insight into the last samples, the magnetization measurements are reported. Fig. 4 shows the hysteresis loop recorded at room temperature for the sample A. This is a typical ferromagnet characterized by small remanence and coercivity. We can also note that the magnetization is far from the saturation

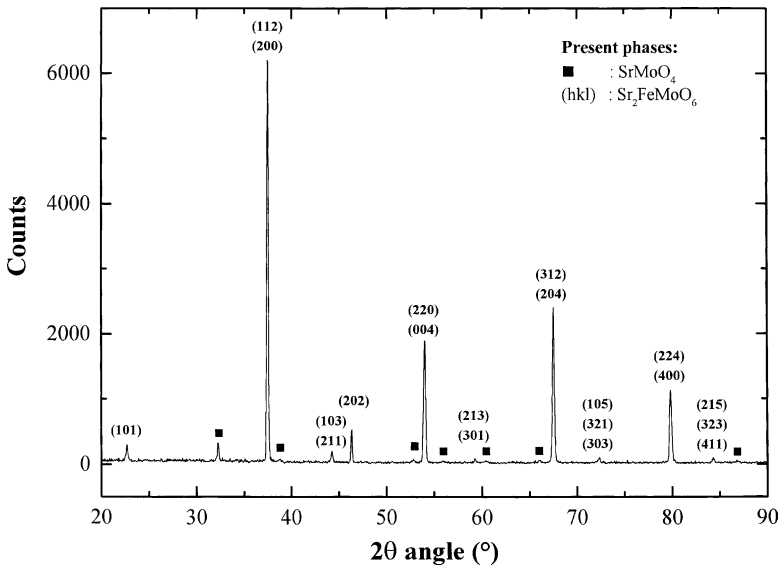

Fig. 2. X-ray diffraction pattern for Sr_2FeMoO_6 sample labeled A recorded at room temperature with Co Kα radiation.

at 1.5 T with a value of 26.7 emu/g (2.03μ_B). This is lower than the expected value of 4μ_B for the ferromagnetic state with the nominal ionic configuration Fe^{3+} ($S = \frac{5}{2}$)/Mo^{5+} ($S = \frac{1}{2}$). Indeed, the Curie temperature of this sample (T_C = 410 K) is only 100 K above room temperature. Therefore, thermal fluctuations are expected to be very important at room temperature, which gives rise to a sensitive reduction of the magnetization with respect to its saturation value at low temperature. However, this value is of the same order than of the Fe (2.2μ_B) but higher than that of Co and Ni (1.7 and 0.6μ_B, respectively). In addition, taking into account the half metallic character of this magnetic oxide, this magnetization value could lead to a high spin polarization, which is very interesting for spintronic devices [6]. Such magnetization value corresponds to the highest value obtained within this synthesis process. Indeed in Fig. 5, various magnetization curves corresponding to different samples prepared at different sintering temperatures are reported. It is clearly seen that the magnetization is very sensitive to the sintering temperature since it varies strongly with increasing the sintering temperature to reach its high value at 1200 °C within this process. In order to have an idea on the quality of this optimized sample we have to look to its magnetization value at low temperature. This is of about 41.6 emu/g (3.15μ_B) at 5 K and 1.5 T and it is still lower than the expected 4μ_B for a perfect sample. This difference, in addition to the large high field susceptibility is a strong indication that there is still disorder in this sample giving rise to antisite defects

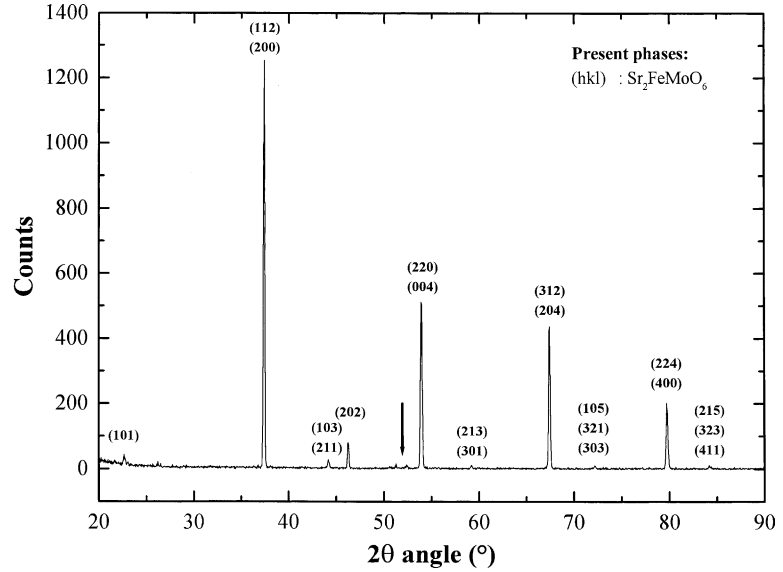

Fig. 3. X-ray diffraction pattern for Sr_2FeMoO_6 sample labeled B recorded at room temperature with Co Kα radiation.

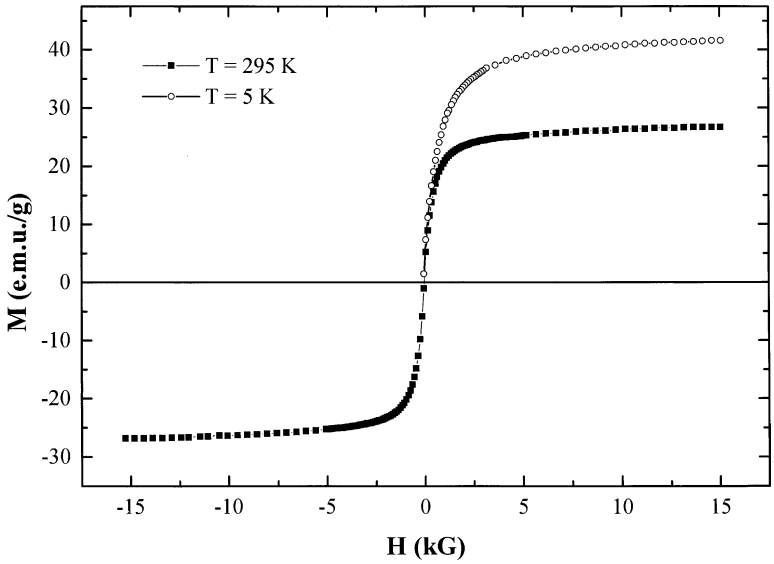

Fig. 4. Magnetization hysteresis loops performed at room temperature (squares) and 5 K (circles) for Sr_2FeMoO_6 sample labeled A.

(randomly misplaced Fe ions at Mo sites and vice versa) or/and antiphase boundaries defects (Fe(Mo)–O planes are substituted by Mo(Fe)–O planes). Both types of defects are expected to induce a significant magnetic frustration as expressed by reduced magnetization value and a large high field susceptibilities. If a Mo^{5+} ($S = \frac{1}{2}$) is at the B_{Fe} site surrounded by the Mo^{5+} neighbors, its magnetic moment tends to be parallel to those of Mo^{5+} ions, which decreases the net magnetization. Inversely, if a Fe^{3+} ($S = \frac{5}{2}$) is at a B_{Mo} site, its magnetic moment tends to be antiparallel to those Fe^{3+} ions, causing to a decrease in the net magnetization.

Fig. 6 shows the magnetization hysteresis loops recorded at low and room temperatures for the perovskite B prepared within the second sintering process. The same ferromagnetic behavior is observed as for the sample A. However, the magnetization at 1.5 T is smaller than the value obtained for the sample A. Indeed we obtain $M_{1.5\,T} = 21$ emu/g ($\propto 1.61\mu_B$) and $M_{1.5\,T} = 40.3$ emu/g ($\propto 3.05\mu_B$). In addition, the high field susceptibility is larger than the value observed for the sample A. Such results are surprising with respect to the X-ray diffraction spectra, which have shown that the sample B presents less impurity phases than the sample A. This indicates that the factor which has more influence on the magnetic properties is not the impurity phases present in the sample but the density of antisite defects and/or antiphase boundaries in the structure.

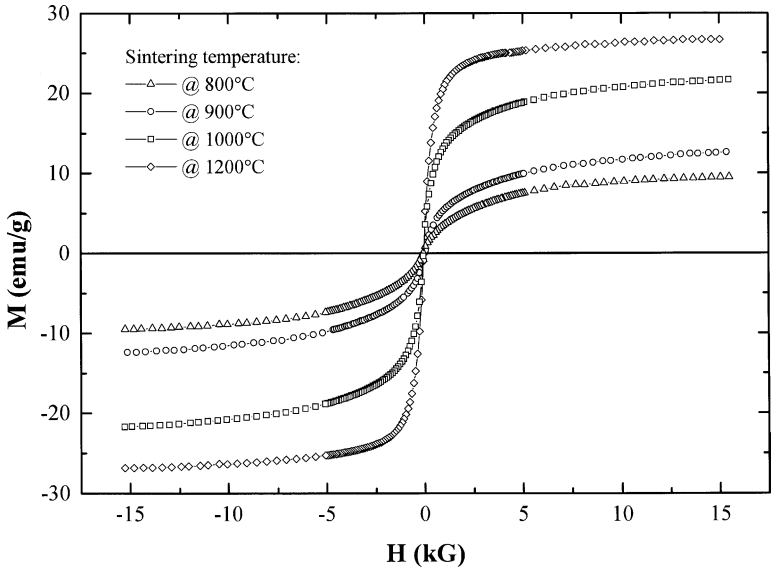

Fig. 5. Magnetization hysteresis loops performed at room temperature for different Sr_2FeMoO_6 sample labeled A sintered at various temperatures 800 °C (triangles), 900 °C (circles), 1000 °C (squares) and 1200 °C (diamonds).

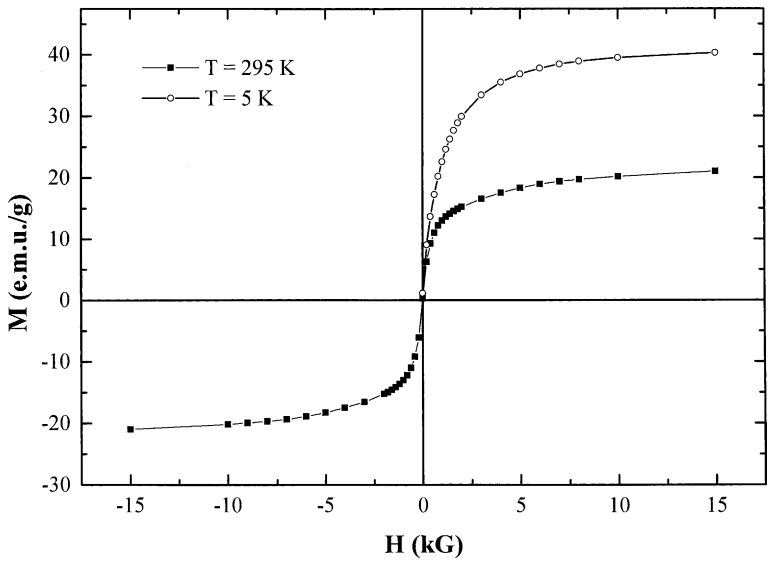

Fig. 6. Magnetization hysteresis loops performed at room temperature (squares) and 5 K (circles) for Sr_2FeMoO_6 sample labeled B.

3.3. Magnetoresistance

In order to support the last results, we report the magnetoresistance measurements. Fig. 7 shows the MR loop recorded for the sample A at room temperature. The total MR reaches 2.5% at the highest field value of 1.2 T allowed by our equipments. This value is not high and is smaller than the values observed for samples prepared by the same sintering process but with less well-defined crystalline quality and with more impurities. This indicates that better the quality of the perovskite is, lower is the value of the MR. Therefore, for a single crystal with large grain sizes, no MR is then expected. The figure also shows that the MR has two contributions: low field and high field contributions. This is in good agreement with all reports on this type of structure [12–14]. Such behavior can be compared with what is usually observed in granular systems [15–17]. The low field MR is correlated to the grain size and consequently to the sintering temperature. Therefore, the sample with the smallest grain size presents the largest surface/volume ratio and should give a larger MR contribution at low field. However, the high field MR contribution is correlated to the disorder and the difficulty to saturate the magnetization. Thus for the sample with the largest disorder, the MR should be higher. Following these analyses, it is then interesting to look at the MR loop recorded for the sample B at room temperature and reported in Fig. 8. First the MR value of this sample is higher and of about 3.9%. Moreover, if we look to the

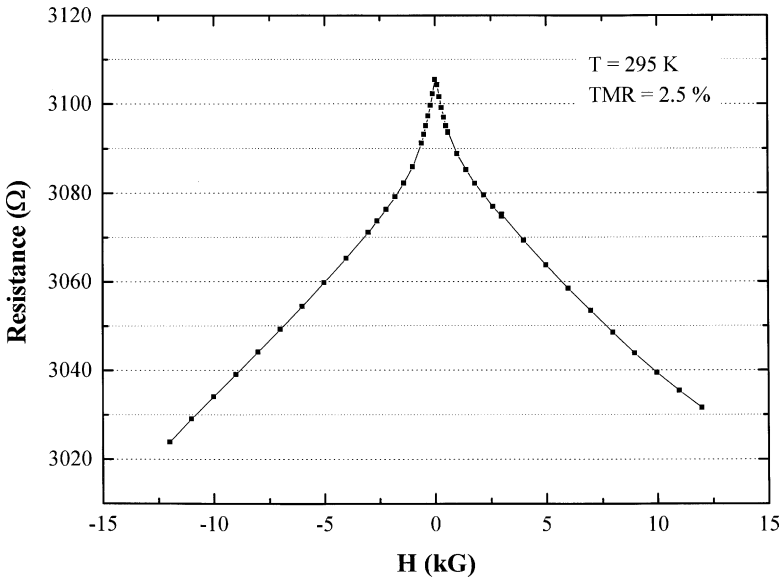

Fig. 7. Magnetoresistance loops performed at room temperature for Sr_2FeMoO_6 sample labeled A.

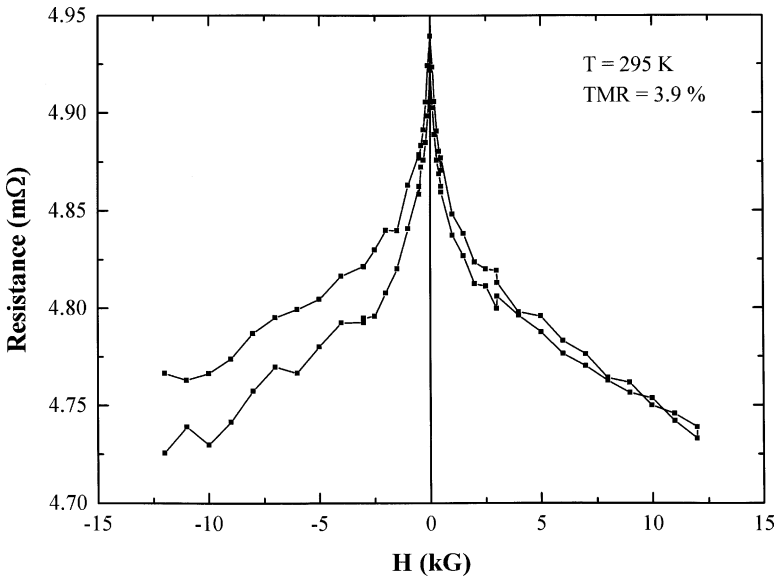

Fig. 8. Magnetoresistance loops performed at room temperature for Sr_2FeMoO_6 sample labeled B.

resistance slopes at low and high fields, we find that both slopes are higher than those for the previous sample A. This indicates that the sample presents more disorder which is in good agreement with the magnetization results. In addition the resistance value for the sample A is few order of magnitude larger than the resistance of the sample B. This means that the presence of the $SrMoO_4$ oxide phase in the sample A increases significantly the resistance of this sample. In addition the conduction mechanism is not the same between the two samples. For the sample A the conduction mechanism is close to what is observed in magnetic tunnel junctions [18,19]. Thus, the conduction electrons are tunneling through the insulating $SrMoO_4$ barrier giving rise to a tunneling magnetoresistance (TMR). However, for the sample B the conduction mechanism is similar to what is observed in granular alloy, which means electron spin dependent diffusion mechanism, giving rise to a giant magnetoresistance (GMR).

4. Conclusion

This work has shown that magnetization and magnetoresistance are a very interesting tool to give an idea on the structural quality of the studied ferromagnetic oxides. Indeed, while the X-ray diffraction has shown that the perovskite elaborated with the second sintering process (sample B) presents less impurity phases than the one from the first sintering process (sample A), the magnetotransport analysis has shown, at the opposite, that the sample A presents a higher order degree than the sample B. Additionally and whatever the elaboration process used, this study underlines all the difficulties encountered to elaborate such a type of structure with the perfect stoichiometry and, therefore, high crystalline quality. This condition is very important for these samples to be used as magnetic electrodes for magnetic tunnel junctions.

References

[1] J. Gregg, J. Magn. Magn. Mater. 175 (1997) 1.
[2] H. Ohno, Science 281 (1998) 951.
[3] G.A. Prinz, Science 282 (1998) 1660.
[4] J.M. Kikkawa, I.P. Smorchkova, N. Samarth, D.D. Awschalom, Science 277 (1997) 1284.
[5] K.I. Kobayashi, T. Kimura, H. Sawada, K. Terakura, Y. Tokura, Nature 395 (1998) 677.
[6] M.F. Hundley, J.H. Nickel, R. Ramesh, Y. Tokura, Science and Technology of Magnetic Oxides, Mater. Res. Soc. Proc. 494 (1998).
[7] A.W. Sleight, J.W. Weiher, J. Phys. Chem. Solids 33 (1972) 679.
[8] A. Ogale, S. Ogale, R. Ramesh, T. Venkatesan, Appl. Phys. Lett. 75 (1999) 537.
[9] L. Blacells, J. Navarro, M. Bibes, A. Roig, B. Martinez, J. Fontcuberta, Appl. Phys. Lett. 78 (2001) 781.
[10] T. Tomika, T. Okuda, Y. Okimoto, R. Kumai, K.I. Kobayashi, Y. Tokura, Phys. Rev. B 61 (2000) 422.
[11] C. Ritter, M.R. Ibarra, L. Morellon, J. Garcia, J.M. De Teresa, J. Phys.: Condens. Matter 12 (2000) 8295.
[12] K.I. Kobayashi, T. Kimura, Y. Tomioka, H. Sawada, K. Terakura, K. Tokura, Phys. Rev. B 59 (1999) 11159.
[13] D. Niebieskikwiat, A. Caneiro, R.D. Sanchez, J. Fontcuberta, Phys. Rev. B 64 (2001) 180406.
[14] H. Yanagihara, M.B. Salamon, Y. Lyanda-Geller, Sh. Xu, Y. Moritomo, Phys. Rev. B 64 (2001) 214407.
[15] A.E. Berkowitz, J.R. Michel, M.J. Carey, A.P. Young, F.E. Spada, F.T. Parker, A. Hutton, G. Thomas, Phys. Rev. Lett. 68 (1992) 3745.
[16] J.Q. Xiao, J.S. Jiang, C.L. Chien, Phys. Rev. Lett. 69 (1992) 3749.
[17] H. Errahmani, A. Berrada, G. Schmerber, A. Dinia, J. Magn. Magn. Mater. 238 (2002) 147.
[18] J.S. Moodera, L.R. Kinder, T.M. Wong, R. Meservey, Phys. Rev. Lett. 74 (1995) 3273;
J.S. Moodera, L.R. Kinder, T.M. Wong, R. Meservey, J. Appl. Phys. 79 (1996) 4724.
[19] M. Guth, A. Dinia, G. Schmerber, H.A.M. van den Berg, Appl. Phys. Lett. 78 (2001) 3487.